

# Approximating Full Conformal Prediction at Scale via Influence Functions

Javier Abad<sup>1</sup> Umang Bhatt<sup>1,2</sup> Adrian Weller<sup>1,2</sup> Giovanni Cherubin<sup>2</sup>

## Abstract

Conformal prediction (CP) is a wrapper around traditional machine learning models, giving coverage guarantees under the sole assumption of exchangeability; in classification problems, for a chosen significance level  $\varepsilon$ , CP guarantees that the number of errors is at most  $\varepsilon$ , irrespective of whether the underlying model is misspecified. However, the prohibitive computational costs of “full” CP led researchers to design scalable alternatives, which alas do not attain the same guarantees or statistical power of full CP. In this paper, we use influence functions to efficiently approximate full CP. We prove that our method is a consistent approximation of full CP, and empirically show that the approximation error becomes smaller as the training set increases; e.g., for  $10^3$  training points the two methods output p-values that are  $< 10^{-3}$  apart: a negligible error for any practical application. Our methods enable scaling full CP to large real-world datasets. We compare our full CP approximation (ACP) to mainstream CP alternatives, and observe that our method is computationally competitive whilst enjoying the statistical predictive power of full CP.

## 1. Introduction

Conformal prediction (CP) is a post-hoc approach to providing validity guarantees on the outcomes of machine learning (ML) models; in classification, an ML model wrapped with “full” CP outputs prediction sets that contain the true label with (chosen) probability  $1 - \varepsilon$ , under mild distribution assumptions. Unfortunately, full CP is notoriously computationally expensive. Many have proposed alternative methods to avoid the full CP objective; these methods include: split (or “inductive”) CP (Papadopoulos et al., 2002a), cross-CP (Vovk, 2015), jackknife+ (Barber et al., 2021),

<sup>1</sup>Department of Engineering, University of Cambridge, UK <sup>2</sup>The Alan Turing Institute, London, UK. Correspondence to: Umang Bhatt <usb20@cam.ac.uk>, Adrian Weller <aw665@cam.ac.uk>.

RAPS (Angelopoulos et al., 2020), and CV+ (Romano et al., 2020). While these methods have shown practical promise, they do not attain the same validity guarantee as full CP or its statistical power (e.g., average prediction set size). Recent work optimized full CP for the family of ML models that support incremental and decremental learning, by speeding up the leave-one-out (LOO) procedure required for the prediction set calculation (Cherubin et al., 2021). However, this approach may not scale to more complex machine learning models such as neural networks.

Herein, we first discuss how to approximate the full CP objective. We focus on full CP for classification, and optimize it for ML models trained via ERM (e.g., logistic regression, neural networks). The key insight we leverage for our method is that, for each test point, full CP: (i) re-trains the underlying ML model on the additional test point, and (ii) performs a LOO procedure for each training point. We observe that we can approximate both steps, and avoid retraining each time, by using first order influence functions (Hampel, 1974). We term our method *Approximate full Conformal Prediction* (ACP), and we prove finite-sample error guarantees: as the training set increases, our approximation approaches exact full CP. We then show that using a stronger regularization parameter for training the underlying ML model further improves the approximation quality.

Empirically, we demonstrate that ACP is competitive with existing methods on MNIST (LeCun, 1998), CIFAR-10, and US Census (Ding et al., 2021). Unlike full CP, ACP can scale to large datasets for a variety of real-world ML models (logistic regression, multilayer perceptrons, and convolutional neural networks). Performance-wise, ACP is consistently better than existing alternatives in terms of statistical power: it attains the desired error rate  $\varepsilon$  with tighter prediction sets. In Figure 1, we show that, unlike other methods, ACP learns smaller prediction sets that still contain the true label for multiple examples in CIFAR-10.

We proceed as follows. We first provide a background on CP (Section 2). After introducing influence functions, we propose our method, ACP (Section 3). We provide a theoretical analysis of ACP (Section 3.2), and experiments on synthetic (Section 4) and real-world data (Section 5).

					
Method	Prediction set	Method	Prediction set	Method	Prediction set
ACP (Ours)	{bird, <b>cat</b> , deer, frog}	ACP (Ours)	{auto, cat, frog, <b>horse</b> , truck}	ACP (Ours)	{cat, deer, <b>frog</b> , horse}
SCP	{bird, deer, frog}	SCP	{auto, deer, frog, truck}	SCP	{cat, deer, dog, <b>frog</b> , horse, truck}
RAPS	{bird, <b>cat</b> , deer, dog, frog}	RAPS	{plane, auto, bird, deer, frog, ship, truck}	RAPS	{cat, deer, dog, <b>frog</b> , horse, truck}
CV+	{bird, <b>cat</b> , deer, dog, frog}	CV+	{plane, auto, deer, frog, <b>horse</b> , truck}	CV+	{cat, deer, dog, <b>frog</b> , horse}

Figure 1. Prediction sets generated by different conformal methods in three examples from CIFAR-10. For a typical significance level  $\varepsilon = 0.2$ , our method (ACP) yields prediction sets that (1) contain the true label and (2) are the smallest. This is because ACP approximates well full CP in large training sets, such as CIFAR-10, inheriting its statistical power.

## 2. Preliminaries

We introduce notation, and give background information on “full” CP. We then introduce influence functions (IF), which will serve as the main tool for our optimization.

### 2.1. Notation and full CP

Consider a training set  $Z = (X, Y) \in (\mathcal{X} \times \mathcal{Y})^N$ . For a test object  $x \in \mathcal{X}$  and a chosen significance level  $\varepsilon \in [0, 1]$ , a CP returns a set  $\Gamma^\varepsilon \subseteq \mathcal{Y}$  that contains  $x$ ’s true label with probability at least  $1 - \varepsilon$ . This guarantee (*validity*) holds for any exchangeable distribution on  $Z \cup \{(x, y)\}$ .

Since the error rate of a CP is guaranteed by validity, a data analyst only needs to control the size of the prediction set  $\Gamma^\varepsilon$ . The *efficiency* is a metric measuring how tight a CP’s prediction set is; e.g., average  $|\Gamma^\varepsilon|$  is a common efficiency metric (Vovk et al., 2016). Efficiency is controlled by improving the underlying ML model that the CP wraps.

**Underlying model.** A CP can be built around virtually any ML model  $\theta$ . We assume the underlying model is trained via ERM, by minimizing the risk function  $R(Z, \hat{\theta}) \equiv \frac{1}{N} \sum_{z_i \in Z} \ell(z_i, \hat{\theta})$ ;  $\ell(z, \theta)$  is the loss of the model at a point  $z$ , and we assume it to be convex and twice differentiable in  $\theta$ . This assumption holds for many popular loss functions. We let  $\theta_Z \equiv \operatorname{argmin}_{\hat{\theta} \in \Theta} R(Z, \hat{\theta})$  be the solution to the ERM optimization problem; we assume this solution to be unique, and discuss relaxations in Section 6.

**Nonconformity measure.** The underlying model is used to construct a nonconformity measure, which defines a CP. A nonconformity measure is a function  $A : (\mathcal{X} \times \mathcal{Y}) \times (\mathcal{X} \times \mathcal{Y})^* \rightarrow \mathbf{R}$  which scores how *conforming* (or *similar*) an example  $(x, y)$  is to a bag of examples  $\bar{Z}$ . In this paper, we focus on the two most common ways of defining nonconformity measures on the basis of an ML model: the *deleted* and the *ordinary* scheme (Vovk et al., 2005).

**Full CP (deleted).** Consider example  $\hat{z}$  and a training set  $Z$ . The nonconformity measure can be defined from the

deleted (LOO) prediction:

$$A(z_i, Z) = \ell(z_i, \theta_{Z \cup \{\hat{z}\} \setminus \{z_i\}}); \quad (1)$$

for all  $z_i \in Z \cup \hat{z}$ . Computing this nonconformity measure requires training the model on dataset  $Z \cup \{\hat{z}\}$ , which we call the *augmented dataset*. This scheme computes the loss at a point after removing it from the model’s training data.

Algorithm 1 shows how the nonconformity measure is used in full CP. For a test point  $x$ , CP runs a statistical test for each possible label  $\hat{y} \in \mathcal{Y}$  to decide if it should be included in the prediction set  $\Gamma^\varepsilon$ . The statistical test requires computing a nonconformity score  $\alpha_i$  by running  $A$  for each point in the augmented training set  $Z \cup \{(x, \hat{y})\}$ ; then, a p-value is computed, and a decision is taken based on the threshold  $\varepsilon$ . This algorithm is particularly expensive. Crucially, for each test point, and for every candidate label, one needs to retrain the underlying ML model  $N + 1$  times.

**Full CP (ordinary).** A computationally faster scheme for defining nonconformity measures based on model  $\theta$  is achieved by taking the loss at the point:

$$A(z_i, Z) = \ell(z_i, \theta_{Z \cup \{\hat{z}\}}). \quad (2)$$

We refer to this as the *ordinary* scheme. Note that this method is inherently faster than the deleted approach, as it only requires training one model per test example. However, the deleted scheme generally leads to less efficient predictions (Section 5). We report the algorithm in Appendix A.

### 2.2. Influence functions

Influence functions (IF) are at the core of our proposal. For a training example  $z_i \in Z$ , let  $I_\theta(z_i) = -\frac{1}{N} H_\theta^{-1} \nabla_\theta \ell(z_i, \theta)$  be the *influence* of  $z_i$  on model  $\theta$ , where  $H_\theta = \nabla^2 R(Z, \theta)$  is the Hessian; by assumption,  $H_\theta$  exists and is invertible. A standard result by Hampel (1974) shows that:

$$\theta_{Z \setminus \{z_i\}} - \theta \approx -I_\theta(z_i). \quad (3)$$

$I_\theta$  says by how much  $\theta$  is affected by  $z_i$  during training. In general, we can apply influence functions for computing the

influence of a point  $z_i$  on any functional. For our purposes, we are particularly interested in the influence on the loss function at a point  $z$ . We define  $I_\ell(z, z_i) = \nabla \ell(z, \theta) I_\theta(z_i)$ . Then, similar to above, we have

$$\ell(z, \theta_{Z \setminus \{z_i\}}) - \ell(z, \theta) \approx -I_\ell(z, z_i). \quad (4)$$

IF have been used in the past for approximating LOO measurements, such as LOO error (Hampel, 1974), and more recently as a way of determining the contribution of individual (or groups of) training examples to a functional (Koh & Liang, 2017; Koh et al., 2019; Giordano et al., 2019).

### 3. Approximate full Conformal Prediction

Our proposal, *Approximate full Conformal Prediction* (ACP), hinges on approximating the nonconformity scores via IF. We describe our approach, and prove theoretical results concerning its consistency and approximation error.

#### 3.1. Approach

The bottleneck of running full CP is the computation of the nonconformity scores  $\alpha_i = \ell(z_i, \theta_{Z \cup \{\hat{z}\} \setminus \{z_i\}})$ . Each score is determined by computing the loss of the model at point  $z_i \in Z \cup \{\hat{z}\}$  after adding point  $\hat{z}$  and removing point  $z_i$  from the model's training data  $Z$ .

There are two ways to approximate  $\alpha_i$  via IF: we can approximate the contribution of adding and removing the points to the learned model  $\theta_Z$ , and then evaluate its loss at  $z_i$  (*indirect* approach), or we can directly approximate the contribution of the points on the loss function (*direct* approach). We describe both below.

**Indirect approach.** We can use Equation 3 to approximate model  $\theta_{Z \cup \{\hat{z}\} \setminus \{z_i\}}$  and then compute its loss. That is, let  $\tilde{\theta}_{Z \cup \{\hat{z}\} \setminus \{z_i\}} \equiv \theta_Z + I_{\theta_Z}(\hat{z}) - I_{\theta_Z}(z_i)$ . Then:

$$\alpha_i \approx \ell(z_i, \tilde{\theta}_{Z \cup \{\hat{z}\} \setminus \{z_i\}}). \quad (5)$$

**Direct approach.** A second approach is to directly compute the influence on the loss. Let  $\theta_Z$  be a model trained via ERM on the entire training set  $Z$ . The direct approximation for the nonconformity score is

$$\alpha_i \approx \tilde{\ell}(z_i, \theta_{Z \cup \{\hat{z}\} \setminus \{z_i\}}) \equiv \ell(z_i, \theta_Z) + I_\ell(z_i, \hat{z}) - I_\ell(z_i, z_i). \quad (6)$$

Here,  $I_\ell(z_i, \hat{z})$  and  $-I_\ell(z_i, z_i)$  are respectively the influence of *including* point  $\hat{z}$  and *excluding*  $z_i$  (Equation 4).

Algorithm 2 (ACP) shows how both approaches enable approximating full CP; both have the same computational cost. In the next part, we show that the direct approach is at least

as good as the indirect one, and we establish conditions under which ACP is a good approximation of full CP.

ACP gives a substantial speed-up over full CP. Differently from full CP, ACP has a training phase, in which we: compute the Hessian, the gradient for each point  $z_i$ , and provisional scores  $\ell(z_i, \theta_Z)$  for  $z_i \in Z$ . For predicting a test point  $\hat{z}$ , it suffice to compute its influence by using the Hessian and gradients at  $z_i$  and  $\hat{z}$ , which is cheap, and update the provisional scores. Thanks to this, ACP can scale to large real-world datasets such as CIFAR-10 (Section 5).

#### 3.2. Theoretical analysis

Hereby, we prove that ACP is a consistent estimator of full CP: its approximation error gets smaller as the training set grows. As a step to consistency, we prove a result which is of independent interest: the direct approximation is better than the indirect; our experiments will focus on the direct approach. Finally, we establish a relation between ACP's approximation and the ERM regularization parameter.

In the following, we make two assumptions.

**Assumption 1.** For every  $z_i \in Z$ :

$$\ell(z_i, \theta_{Z \cup \{\hat{z}\} \setminus \{z_i\}}) \leq \ell(z_i, \theta_Z).$$

This says that a model trained on dataset  $Z$  (s.t.  $z_i \in Z$ ) has a smaller loss at  $z_i$  than a model that is not trained on  $z_i$ .

**Assumption 2.** For every  $z_i \in Z$ :

$$I_\ell(z_i, \hat{z}) \geq I_\ell(z_i, z_i).$$

This assumption can be derived from two basic assumptions. First, observe that  $I_\ell(z_i, z_i) \leq 0$ ; the reason is that removing  $z_i$  from the training set of the model will increase the model's loss at  $z_i$ . (Note that this is analogous to the observation made for Assumption 1, although that assumption applies to the real effect and not to the IF approximation.) Second, the effect *on the loss at  $z_i$*  of adding/removing a training point  $z_i$  is stronger in magnitude than adding/removing point  $\hat{z}$ ; that is,  $|I_\ell(z_i, z_i)| \geq |I_\ell(z_i, \hat{z})|$ .

#### DIRECT APPROXIMATION IS BETTER THAN INDIRECT

We first prove that the direct approximation gives better approximations than the indirect method.

**Lemma 1.** Assume that the loss  $\ell$  is convex and differentiable. Let  $\alpha_i = \ell(z_i, \theta_{Z \cup \{\hat{z}\} \setminus \{z_i\}})$ . Then:

$$|\tilde{\ell}(z_i, \theta_{Z \cup \{\hat{z}\} \setminus \{z_i\}}) - \alpha_i| \leq |\ell(z_i, \tilde{\theta}_{Z \cup \{\hat{z}\} \setminus \{z_i\}}) - \alpha_i|.$$

That is, the direct method (Equation 6) gives a better approximation than the indirect one (Equation 5).

All proofs are deferred to Appendix B. In Section 4, we confirm this result on synthetic data. From now on, we focus our attention on the direct approach.

**Algorithm 1** Full CP

```

1: for  $x$  in test points do
2:   for  $\hat{y} \in \mathcal{Y}$  do
3:      $\hat{z} = (x, \hat{y})$ 
4:     for  $z_i \in Z \cup \{\hat{z}\}$  do
5:        $\theta_{Z \cup \{\hat{z}\} \setminus \{z_i\}} = \operatorname{argmin}_{\hat{\theta} \in \Theta} R(Z \cup \{\hat{z}\} \setminus \{z_i\}, \hat{\theta})$ 
6:        $\alpha_i = \ell(z_i, \theta_{Z \cup \{\hat{z}\} \setminus \{z_i\}})$ 
7:     end for
8:      $p_{(x, \hat{y})} = \frac{\#\{i=1, \dots, N+1 : \alpha_i \geq \alpha_{N+1}\}}{N+1}$ 
9:     If  $p_{(x, \hat{y})} > \varepsilon$ , include  $\hat{y}$  in prediction set  $\Gamma^\varepsilon$ 
10:   end for
11: end for

```

**Algorithm 2** Approximate full CP (ACP)

```

1:  $\theta_Z = \operatorname{argmin}_{\hat{\theta} \in \Theta} R(Z, \hat{\theta})$ 
2: for  $x$  in test points do
3:   for  $\hat{y} \in \mathcal{Y}$  do
4:      $\hat{z} = (x, \hat{y})$ 
5:     for  $z_i \in Z \cup \{\hat{z}\}$  do
6:        $\tilde{\alpha}_i = \text{Approximate via Equation 5 or 6}$ 
7:     end for
8:      $p_{(x, \hat{y})} = \frac{\#\{i=1, \dots, N+1 : \tilde{\alpha}_i \geq \tilde{\alpha}_{N+1}\}}{N+1}$ 
9:     If  $p_{(x, \hat{y})} > \varepsilon$ , include  $\hat{y}$  in prediction set  $\Gamma^\varepsilon$ 
10:   end for
11: end for

```

Figure 2. Full CP (left) and our proposal, ACP, (right). In ACP, the underlying ML model is only trained once, and nonconformity scores are approximated via influence functions in Line 6.

**CONSISTENCY OF ACP**

We show under mild conditions that our method is a consistent estimator of full CP. We establish this equivalence in the most generic form possible: we demonstrate that the nonconformity scores produced by Algorithm 2 approximate those produced by full CP. In turn, this implies that the p-values of the two methods get increasingly closer, which means that ACP inherits the guarantees of full CP.

Our result exploits the work by Giordano et al. (2019), who showed that IF consistently estimate a model’s parameters in a LOO setting. We make the following assumptions, which Giordano et al. (2019) showed to hold under uniform convergence under reasonable data-generating distributions:

**Assumption 3.**

- For all  $\theta \in \Theta$  and all  $z_i \in Z$ ,  $\nabla_\theta \ell(z_i, \theta)$  is continuously differentiable in  $\theta$ .
- For all  $\theta \in \Theta$ , the Hessian  $H_\theta$  is non-singular with  $\sup_{\theta \in \Theta} \|H_\theta^{-1}\|_{op} \leq C_{op} < \infty$ .
- $\exists$  finite constants  $C_g, C_h$  s.t.  $\sup_{\theta \in \Theta} \frac{1}{\sqrt{N}} \|\nabla_\theta \ell(z, \theta)\|_2 \leq C_g$  and  $\sup_{\theta \in \Theta} \frac{1}{\sqrt{N}} \|\nabla_\theta^2 \ell(z, \theta)\|_2 \leq C_h$ .
- Let  $h(\theta) = \nabla_\theta^2 \ell(z, \theta)$ . There exists  $\Delta_\theta > 0$  and a finite constant  $L_h$  such that  $\|\theta - \theta_Z\|_2 \leq \Delta_\theta$  implies that  $\frac{\|h(\theta) - h(\theta_Z)\|_2}{\sqrt{N}} \leq L_h \|\theta - \theta_Z\|_2$ .

Let  $\alpha_i = \ell(z_i, \theta_{Z \cup \{\hat{z}\} \setminus \{z_i\}})$ . Assuming the above, we have:

**Theorem 2** (Consistency of approximate full CP). *Suppose  $\ell$  is  $K$ -Lipschitz. Then for every  $N$  there is a constant  $C$  such that for every  $z_i \in Z \cup \{\hat{z}\}$ :*

$$|\tilde{\ell}(z_i, \theta_{Z \cup \{\hat{z}\} \setminus \{z_i\}}) - \alpha_i| \leq KC \frac{\max\{C_g, C_h\}^2}{N}.$$

This result gives a finite-sample bound for the error of the direct approach for ACP; the error of the indirect approach is also bounded as a byproduct of the same proof. We conclude that, as  $N$  grows, ACP’s scores get increasingly closer to those produced by full CP. We evaluate this in Section 4.

**RELATION TO REGULARIZATION PARAMETER**

By exploiting results by Koh et al. (2019), we investigate how the ERM regularization parameter affects the goodness of our methods at approximating full CP. This result makes fairly simplistic assumptions discussed in Appendix B.3.

Suppose the underlying ML model is trained via  $L_2$ -regularized ERM, for some regularization parameter  $\lambda > 0$ .

**Theorem 3** (Approximation goodness w.r.t. regularizer).

*Suppose the model is trained via ERM with regularization parameter  $\lambda$ . Under the assumptions of Proposition 5, Assumption 4, and neglecting  $\mathcal{O}(\lambda^{-3})$  terms, we have the following cone constraint between the true nonconformity measure  $\alpha_i = \ell(z_i, \theta_{Z \cup \{\hat{z}\} \setminus \{z_i\}})$  and its direct approximation  $\tilde{\ell}(z_i, \theta_{Z \cup \{\hat{z}\} \setminus \{z_i\}}) \equiv \ell(z_i, \theta_Z) + I_\ell(z_i, \hat{z}) - I_\ell(z_i, z_i)$ :*

$$\ell(z_i, \theta_Z) + I_\ell(z_i, \hat{z}) - g(\lambda) I_\ell(z_i, z_i) \leq \alpha_i \leq \tilde{\ell}(z_i, \theta_{Z \cup \{\hat{z}\} \setminus \{z_i\}})$$

with  $g(\lambda) = (1 + 3\sigma_{max}/2\lambda + \sigma_{max}^2/2\lambda^2)$ , where  $\sigma_{max}$  is the maximum eigenvalue of the Hessian  $H$ .

This theorem tells us that a stronger regularization implies ACP approximates full CP better.

**4. Experiments on synthetic data**

We generate synthetic data for a binary classification problem using scikit-learn’s `make_classification()` (Pe-

dregosa et al., 2011). We sample points from four Gaussian-distributed clusters (two per class) and fit a logistic regression model. We investigate the properties of ACP outlined in Section 3.2. All results are reported for 100 test points.

#### 4.1. Direct and indirect approximation

We empirically evaluate Lemma 1, which claims that the direct method (Equation 6) is never worse than the indirect method (Equation 5). We confirm this result, by plotting the absolute distance between full CP nonconformity scores and ACP’s scores as a function of the training set size (Figure 3). We observe that the direct approach is always better than the indirect one, although the two get closer for large  $N$ . Importantly, this also shows that the nonconformity scores produced by ACP get increasingly better at approximating those of full CP as the training set grows (cf. Theorem 2). We focus our experiments on the direct approach.

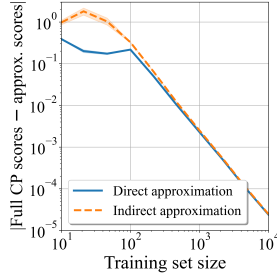


Figure 3. Comparison between the direct and indirect approximation. We show the difference between the nonconformity scores of full CP and their approximation as a function of the training set size, averaged across 100 test points. The empirical results support that the direct method is never worse than the indirect, and that both asymptotically produce the same nonconformity scores.

#### 4.2. Approximation goodness

We evaluate how well ACP approximates full CP, as the training set size increases, under various parameter choices.

**Number of features.** In Figure 4a, we measure the difference between the nonconformity measures of full CP and ACP as the number of features ranges in 5 – 100. Results show that the number of features does impact the influence function approximation, although the error becomes negligible as the training set increases.

**Regularization strength.** Theorem 3 shows that the regularization parameter  $\lambda$  plays an important role: a larger  $\lambda$  (i.e., stronger regularization) implies better approximation. We confirm this in Figure 4b.

**Nonconformity scores and p-values.** Our analysis focuses on the approximation error between nonconformity

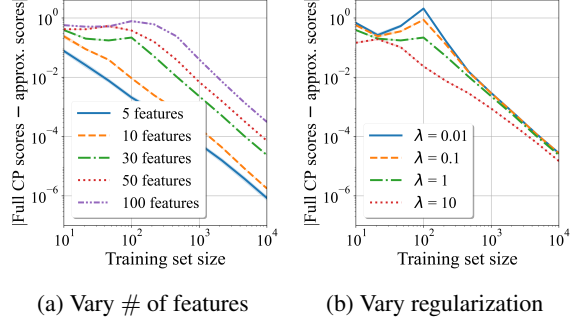


Figure 4. Difference in nonconformity scores for different numbers of features (4a) and for different regularization strengths (4b). The differences in scores are averaged across 100 test points.

scores. Indeed, we observe that a small error between scores implies a more fundamental equivalence between full CP and ACP: their p-values should also have a small distance, and, consequently, ACP inherits validity from full CP.

Figure 5a shows the difference between full CP and ACP in terms of p-values. The difference becomes negligible with  $N = 10,000$  training examples, and it becomes smaller than  $10^{-3}$  with a training set of 600.

Observe that in CP the p-value is thresholded by the significance value  $\varepsilon$  to obtain a prediction (Algorithm 1). As practitioners are generally interested in values  $\varepsilon$  with no more than 2 decimals of precision (e.g.,  $\varepsilon = 0.15$ ), we argue that an approximation error smaller than  $10^{-3}$  between p-values is more than sufficient for any practical application. Figure 5b compares the measured error (for  $\varepsilon = 0.1$ ) between full CP and ACP. We observe that, after roughly 500 training points, the two methods give the same error.

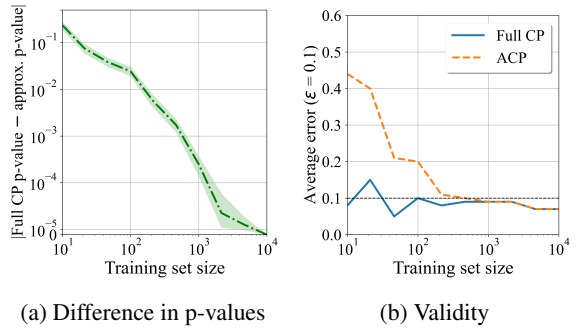


Figure 5. Difference between full CP’s and ACP’s p-values (5a) and error rate (i.e., average rate at which the true label is not in the prediction set) (5b), as a function of the training set size. The approximate p-values exactly match full CP for  $N = 10,000$ .

## 5. Experiments with real data

We now evaluate ACP on real-world data. We discuss mainstream CP alternatives, and compare them empirically with

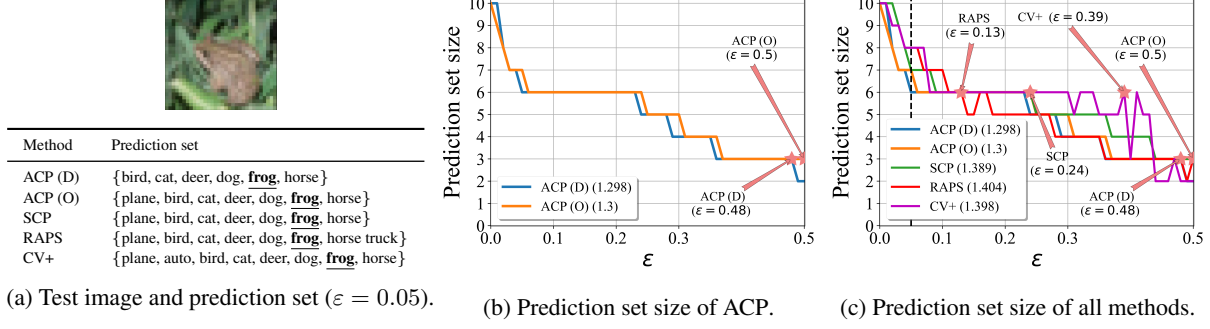


Figure 6. Prediction set for a fixed significance level ( $\varepsilon = 0.05$ ) (a), and prediction set size for a varying  $\varepsilon$  for ACP (b), and for ACP and the comparing methods (c). For each method,  $\star$  indicates the highest  $\varepsilon$  for which the prediction set includes the true label; higher is better. We indicate the AUC in the interval  $\varepsilon \in [0, 0.2]$  in the legend; lower is better (more efficient).

ACP on the basis of their predictive power (efficiency). Because of its computational complexity, it is infeasible to run full CP on the datasets used in these experiments. Nevertheless, given the size of the training data, consistency of ACP (Theorem 2), and results in Section 4.2, we expect ACP to perform similarly to what we would get via full CP.

### 5.1. Existing alternatives to Full CP

There are several alternative approaches to CP for classification. In this work, we compare ACP with:

- Split (or “inductive”) Conformal Prediction (SCP) (Papadopoulos et al., 2002a;b) works by dividing the training set into *proper training set* and *calibration set*. The model is fit on the proper training set, and the calibration set is used to compute the nonconformity scores.
- Regularized Adaptive Prediction Sets (RAPS) (Angelopoulos et al., 2020), is a regularized version of Adaptive Prediction Sets (APS) (Romano et al., 2020). APS constructs *Generalized inverse quantile conformity scores* from a calibration set adaptively w.r.t. the data distribution. RAPS uses regularization to minimize the prediction set size while satisfying validity.
- Cross-validation+ (CV+) (Romano et al., 2020) exploits a cross-validation approach while constructing the conformity scores similarly to APS. This way, CV+ does not lose predictive power due to a data-splitting procedure, but it is computationally more expensive.

**Datasets.** We compare the methods on three publicly available datasets: MNIST (LeCun, 1998), CIFAR-10, and New York’s 2018 income data from the US Census (Ding et al., 2021); a description of each can be found in Appendix C.1. We selected these datasets to illustrate the performance of ACP in multiple scenarios: a simple classification problem with images (MNIST), a more complex

setting (CIFAR-10), and a binary classification with tabular data (US Census).

### 5.2. A motivating example

We first run an initial motivating experiment for one test point on CIFAR-10. We consider a neural network (NN) with three layers of 100, 50, and 20 neurons. We refer to this network as 100-50-20; Appendix C.2 gives implementation details. We run ACP on this model to predict a test example picked uniformly at random from CIFAR-10.

Figure 6a shows the prediction set for a fixed  $\varepsilon = 0.05$ ; we observe that, while all the methods output the true label, the prediction set of ACP (deleted) is the tightest (i.e., more efficient). We also report how the prediction set size changes w.r.t.  $\varepsilon$ , for ACP (Figure 6b) and for all methods (Figure 6c). As a way of comparing the curves, we include the AUC for the interval  $\varepsilon \in [0, 0.2]$ ; limiting the significance level to this interval captures settings that are generally of practical interest. ACP (deleted and ordinary) have the smallest AUC; follows SCP, CV+, and then RAPS. In the next section, we further investigate why CV+ and RAPS are less efficient. Finally, for each method we report the highest  $\varepsilon$  for which the prediction set contains the true label. A higher value indicates that, for this test example, the method would still be accurate with larger  $\varepsilon$ , which would correspond to tighter prediction sets. Once again, ACP (deleted and ordinary) have the largest values (0.48 and 0.5); follow CV+, SCP, and RAPS (0.13). Notably, ACP includes the true label when the prediction set has size 3, while the rest of the methods do not include it until twice this size. We conclude that ACP is more efficient and accurate for this test point; we show similar instances in Appendix E.2. In the next part, we observe this behavior generalizes to larger test sets.

We observe an unstable behavior in the predictions of RAPS and CV+: their prediction set size considerably oscillates as  $\varepsilon$  increases. The reason is that their prediction sets are not guaranteed to be nested; that is,  $\varepsilon > \varepsilon'$  does not imply that

the prediction sets  $\Gamma^\varepsilon \subseteq \Gamma^{\varepsilon'}$ . Specifically, because RAPS and CV+ use randomness to decide whether to include a label in the set, the true label may appear and then disappear for a smaller significance level. This may not be desirable in some practical applications.<sup>1</sup> The prediction set for ACP and SCP monotonically decreases with  $\varepsilon$ , by construction.

### 5.3. Experimental setup

We evaluate the methods for five underlying ML models: three configurations of neural networks (settings 20-10, 100, and 100-50-20, indicating their width and depth), a logistic regression model (LR), and a convolutional neural network (CNN). In experiments with MNIST and CIFAR-10, the dimensionality is first reduced with an autoencoder (AE) in all settings except the CNN. Different settings use different AE embedding sizes. We defer implementation details and design choices for each method to Appendix C.2-C.3.

Considering these five settings enables comparing the methods both for underparametrized regimes (e.g., LR) and for better performing models (e.g., CNN). Note that CP’s guarantees hold regardless of whether the underlying model is misspecified. Further, observe that most of these models are non-convex, where the ERM optimization problem does not have a unique solution; this contradicts the IF assumption (Section 2). Nonetheless, our empirical results show that ACP works well – it performs better than the other proposals; in Section 6 we discuss relaxations of this assumption.

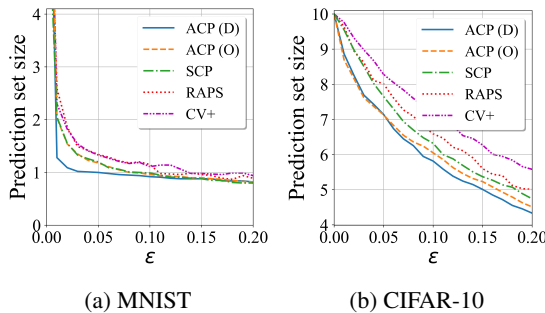


Figure 7. Average prediction set size as a function of the significance level  $\varepsilon$  in MNIST (7a) and CIFAR-10 (7b) for setting 100-50-20. Smaller prediction set size indicates better efficiency.

## 5.4. Results

For each experiment and method, we report averaged metrics over 100 test points; we also run statistical tests to check if differences are (statistically) significant.

**Prediction set size.** We measure efficiency as the average prediction set size. We report this metric as a function of

<sup>1</sup>RAPS allows a non-randomized version, although with a more conservative behavior and considerably larger prediction sets.

US Census					
Model	ACP (D)	ACP (O)	SCP	RAPS	CV+
<b>20-10</b>	0.301	<b>0.281</b>	0.302 <sup>†</sup>	0.318 <sup>*,†</sup>	0.374 <sup>*,†</sup>
<b>100</b>	0.306	<b>0.304</b>	0.351 <sup>*,†</sup>	0.351 <sup>*,†</sup>	0.377 <sup>*,†</sup>
<b>100-50-20</b>	<b>0.273</b>	0.275	0.280	0.299 <sup>*,†</sup>	0.324 <sup>*,†</sup>
<b>LR</b>	0.276	0.276	0.284 <sup>*,†</sup>	<b>0.183</b>	0.344 <sup>*,†</sup>
MNIST					
Model	ACP (D)	ACP (O)	SCP	RAPS	CV+
<b>20-10</b>	<b>0.252</b>	0.253	0.261	0.299 <sup>*,†</sup>	0.322 <sup>*,†</sup>
<b>100</b>	<b>0.220</b>	0.230	0.233	0.266 <sup>*,†</sup>	0.277 <sup>*,†</sup>
<b>100-50-20</b>	<b>0.198</b>	0.231	0.230 <sup>*</sup>	0.258 <sup>*,†</sup>	0.267 <sup>*,†</sup>
<b>LR</b>	0.385	0.386	<b>0.379</b>	0.438 <sup>*,†</sup>	0.467 <sup>*,†</sup>
<b>CNN</b>	<b>0.175</b>	0.182	0.237 <sup>*,†</sup>	0.197 <sup>*,†</sup>	0.199 <sup>*,†</sup>
CIFAR-10					
Model	ACP (D)	ACP (O)	SCP	RAPS	CV+
<b>20-10</b>	1.261	<b>1.259</b>	1.281 <sup>*,†</sup>	1.311 <sup>*,†</sup>	1.373 <sup>*,†</sup>
<b>100</b>	1.385	<b>1.364</b>	1.397 <sup>†</sup>	1.416 <sup>*,†</sup>	1.514 <sup>*,†</sup>
<b>100-50-20</b>	<b>1.226</b>	1.250	1.327 <sup>*,†</sup>	1.377 <sup>*,†</sup>	1.475 <sup>*,†</sup>
<b>LR</b>	1.409	1.411	1.419	1.436 <sup>*,†</sup>	1.476 <sup>*,†</sup>
<b>CNN</b>	<b>0.976</b>	1.108	1.019	1.110 <sup>*</sup>	1.467 <sup>*,†</sup>

Table 1. Efficiency AUC ( $\varepsilon \in [0, 0.2]$ ). The table indicates that differences in the AUC score are statistically significant as compared to ACP (D) (\*) and ACP (O) (†).

$\varepsilon \in [0, 1]$ , discretized with a step  $\Delta\varepsilon = 0.01$ ; each number is obtained by averaging the size across 100 points.

Figure 7a and Figure 7b show the average prediction set size for the MNIST and CIFAR-10 datasets, for a 100-50-20 neural network. Results show that ACP (deleted and ordinary) consistently outperform all other methods; deleted is better than ordinary, although more computationally expensive (Appendix A). The average size of ACP is significantly smaller than for RAPS and CV+. SCP and ACP (O) perform similarly on MNIST, but their difference is more remarked on CIFAR-10; this suggests that SCP may be a cheap effective alternative to ACP on relatively easier datasets. Appendix E.3 reports results for the rest of the models and for the US census, which show a similar behavior.

**Efficiency AUC.** We use an  $\varepsilon$ -independent metric to facilitate comparison between the methods: we measure the area under the curve (AUC) of the prediction set size in the interval  $\varepsilon \in [0, 0.2]$ . A smaller AUC implies a better efficiency. Table 1 illustrates the results. ACP (either deleted or ordinary) prevails on all methods, datasets, and models combinations. An exception is logistic regression on the US Census, where RAPS has a better efficiency than ACP and SCP; this indicates that simpler tasks (datasets) and models may be well served by the computationally efficient RAPS. We run Welch one-sided tests (reject with p-value  $< 0.1$ ), which confirm that both deleted and ordinary ACP are better than RAPS and CV+. They also indicate that either deleted or ordinary ACP are better than SCP on most tasks. We refer to Section 6 for further improvements to push ACP’s per-

formance, such as using a middle way between deleted and ordinary CP. Overall, results suggest that the deleted scheme is more efficient, alas more computationally expensive.

**Validity.** As a way of interpreting why ACP performed better than the other methods, we measure their empirical error rate. Indeed, whilst all methods guarantee a probability of error of at most  $\varepsilon$ , a more conservative (i.e., smaller) empirical error may correspond to very large prediction sets. Figure 8 shows this for the CIFAR-10 dataset. We observe that ACP achieves an error rate close to the significance level in all cases; this indicates this method fully exploits its error margin to optimize efficiency.<sup>2</sup> SCP shows a similar behavior. On the other hand, RAPS and CV+ are more conservative and tend to commit fewer errors. This means that RAPS and CV+ generate unnecessarily large prediction sets that, despite including the true label on average, result in lower efficiency. This behavior is consistent with analogous experiments on the US Census and MNIST datasets.

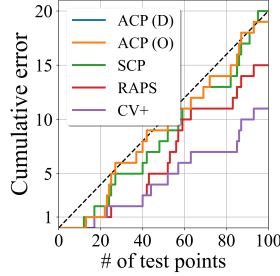


Figure 8. Cumulative error of the methods ( $\varepsilon = 0.2$ ) on CIFAR-10, as a function of test examples coming one by one. Dashed line indicates the expected maximum error rate according to the validity guarantee. All methods have an error rate lower than  $\varepsilon$ . However, RAPS and CV+ are particularly conservative, which explains their lower prediction set efficiency. The lines of ACP (D) and ACP (O) overlap. Since this is based on a small test set of 100 points, it is normal for the error rate to sometimes exceed  $\varepsilon$ .

**P-values fuzziness.** Average prediction set size is a coarse criterion of efficiency (Vovk et al., 2016): a small variation within the algorithm may lead to a substantially different prediction set. An alternative criterion for comparing CP methods is fuzziness, which measures how p-values distribute across the label space. Of the methods we considered, fuzziness can only be measured for ACP and SCP; neither RAPS nor CV+ produce intermediate p-values. Fuzziness is defined as follows: for every test point  $x$ , and computed p-values  $\{p_{(x,\hat{y})}\}_{\hat{y} \in \mathcal{Y}}$ , fuzziness is the sum of the p-values minus the largest p-value:  $\sum_{\hat{y} \in \mathcal{Y}} p_{(x,\hat{y})} - \max_{\hat{y} \in \mathcal{Y}} p_{(x,\hat{y})}$ . A smaller fuzziness is desirable.

<sup>2</sup>Note a randomized version of full CP, called smooth CP, ensures the error rate is exactly  $\varepsilon$  (instead of “at most  $\varepsilon$ ”). Herein, we use the standard, conservatively valid definition per Algorithm 1.

Model	MNIST			CIFAR-10		
	ACP (D)	ACP (O)	SCP	ACP (D)	ACP (O)	SCP
20-10	0.057	0.059	0.068*	1.796	1.832	1.849
100	0.032	0.041	0.043*	1.967	2.050	2.132*
100-50-20	0.012	0.040	0.044*	1.728	1.843	1.878*
LR	0.187	0.189	0.183	2.269	2.280	2.332
CNN	0.002	0.002	0.002	1.186	1.645	1.235

Table 2. Fuzziness of ACP and SCP on MNIST and CIFAR-10. A smaller fuzziness corresponds to more efficient prediction sets.

\*Differences in the AUC score are statistically significant compared to ACP (D).

†Differences are significant compared to ACP (O).

In Table 2, we observe that ACP (D) consistently has a better fuzziness than ACP (O) and SCP. We observe statistical significance of the results for 3 models in MNIST, and 2 models in CIFAR-10. Results for the US Census (Appendix D) are similar. As previously observed in Table 1, SCP performs better in logistic regression (MNIST); this makes it a good alternative for simpler underlying models.

## 6. Conclusion and Future Work

Full CP is a statistically sound method for providing performance guarantees on the outcomes of ML models. For classification tasks, CP enables us to generate a prediction set which contains the true label with a user-specified probability. Unfortunately, full CP is impractical to run for more than a few hundred training points. In this work, we develop ACP, a computationally efficient full CP approximation which avoids numerous recalculations that full CP requires. We prove that ACP is consistent: it approaches full CP as the training set grows. Our synthetic and real-world data experiments support the use of ACP in practice.<sup>3</sup>

There are many directions to pursue in future work to further improve the approximation quality of our methods, such as considering higher order influence functions (Basu et al., 2020). Also, we assumed that the ERM solution is unique. While our approximation works well in practice, it would be a fruitful endeavour to relax this uniqueness assumption; initial work towards this was done for IF by Koh & Liang (2017). Another direction to improve ACP is to build non-conformity measures on the *studentized* scheme, a middle way between deleted and ordinary (Vovk et al., 2017).

Finally, while we do scale full CP to fairly large models with many parameters, computing and inverting the Hessian becomes very expensive as the number of parameters increases. Tools like the Woodbury Identity (Woodbury, 1950) or Hessian-Vector-Products (Pearlmutter, 1994) might help further scale ACP to even larger models like ResNets.

Nevertheless, we reiterate that ACP is a practical tool which

<sup>3</sup>The code will be released at <https://github.com/cambridge-mlg/acp>

helps scale full CP to real-world tasks and ML models. We hope our work will enable evaluations of statistical properties of full CP on large datasets, and can facilitate the adoption of CP methods in real-world critical applications.

## Acknowledgments

UB acknowledges support from DeepMind and the Leverhulme Trust via the Leverhulme Centre for the Future of Intelligence (CFI), and from the Mozilla Foundation. AW acknowledges support from a Turing AI Fellowship under grant EP/V025379/1, The Alan Turing Institute, and the Leverhulme Trust via CFI. GC acknowledges support from The Alan Turing Institute. The authors are grateful to Volodya Vovk for useful comments and pointers.

## References

Angelopoulos, A. N., Bates, S., Jordan, M., and Malik, J. Uncertainty sets for image classifiers using conformal prediction. In *International Conference on Learning Representations*, 2020.

Barber, R. F., Candes, E. J., Ramdas, A., and Tibshirani, R. J. Predictive inference with the jackknife+. *The Annals of Statistics*, 49(1):486–507, 2021.

Basu, S., You, X., and Feizi, S. On second-order group influence functions for black-box predictions. In *International Conference on Machine Learning*, pp. 715–724. PMLR, 2020.

Bhatt, U., Weller, A., and Cherubin, G. Fast conformal classification using influence functions. In Carlsson, L., Luo, Z., Cherubin, G., and An Nguyen, K. (eds.), *Proceedings of the Tenth Symposium on Conformal and Probabilistic Prediction and Applications*, volume 152 of *Proceedings of Machine Learning Research*, pp. 303–305. PMLR, 08–10 Sep 2021.

Cherubin, G., Chatzikokolakis, K., and Jaggi, M. Exact optimization of conformal predictors via incremental and decremental learning. In Meila, M. and Zhang, T. (eds.), *Proceedings of the 38th International Conference on Machine Learning*, volume 139 of *Proceedings of Machine Learning Research*, pp. 1836–1845. PMLR, 18–24 Jul 2021.

Ding, F., Hardt, M., Miller, J., and Schmidt, L. Retiring adult: New datasets for fair machine learning. In Beygelzimer, A., Dauphin, Y., Liang, P., and Vaughan, J. W. (eds.), *Advances in Neural Information Processing Systems*, 2021.

Giordano, R., Stephenson, W., Liu, R., Jordan, M., and Broderick, T. A swiss army infinitesimal jackknife. In *The 22nd International Conference on Artificial Intelligence and Statistics*, pp. 1139–1147. PMLR, 2019.

Hampel, F. R. The influence curve and its role in robust estimation. *Journal of the american statistical association*, 69(346):383–393, 1974.

Koh, P. W. and Liang, P. Understanding black-box predictions via influence functions. In *International Conference on Machine Learning*, pp. 1885–1894. PMLR, 2017.

Koh, P. W. W., Ang, K.-S., Teo, H., and Liang, P. S. On the accuracy of influence functions for measuring group effects. In *Advances in Neural Information Processing Systems*, pp. 5254–5264, 2019.

LeCun, Y. The mnist database of handwritten digits. <http://yann.lecun.com/exdb/mnist/>, 1998.

Linusson, H., Johansson, U., Boström, H., and Löfström, T. Efficiency comparison of unstable transductive and inductive conformal classifiers. In *AIAI Workshops*, 2014.

Papadopoulos, H., Proedrou, K., Vovk, V., and Gammerman, A. Inductive confidence machines for regression. In Elomaa, T., Mannila, H., and Toivonen, H. (eds.), *Machine Learning: ECML 2002*, Berlin, Heidelberg, 2002a. Springer Berlin Heidelberg.

Papadopoulos, H., Vovk, V., and Gammerman, A. Qualified prediction for large data sets in the case of pattern recognition. pp. 159–163, 01 2002b.

Pearlmutter, B. A. Fast exact multiplication by the hessian. *Neural computation*, 6(1):147–160, 1994.

Pedregosa, F., Varoquaux, G., Gramfort, A., Michel, V., Thirion, B., Grisel, O., Blondel, M., Prettenhofer, P., Weiss, R., Dubourg, V., Vanderplas, J., Passos, A., Cournapeau, D., Brucher, M., Perrot, M., and Duchesnay, E. Scikit-learn: Machine learning in Python. *Journal of Machine Learning Research*, 12:2825–2830, 2011.

Romano, Y., Sesia, M., and Candes, E. Classification with valid and adaptive coverage. *Advances in Neural Information Processing Systems*, 33:3581–3591, 2020.

Vovk, V. Cross-conformal predictors. *Annals of Mathematics and Artificial Intelligence*, 74(1):9–28, 2015.

Vovk, V., Gammerman, A., and Shafer, G. *Algorithmic learning in a random world*. Springer Science & Business Media, 2005.

Vovk, V., Fedorova, V., Nouretdinov, I., and Gammerman, A. Criteria of efficiency for conformal prediction. In *Symposium on conformal and probabilistic prediction with applications*, pp. 23–39. Springer, 2016.

Vovk, V., Shen, J., Manokhin, V., and Xie, M.-g. Non-parametric predictive distributions based on conformal prediction. In *Conformal and Probabilistic Prediction and Applications*, pp. 82–102. PMLR, 2017.

Woodbury, M. A. Inverting modified matrices. Statistical Research Group, Memo. Rep. 42, Princeton University, Princeton, N. J, 1950.

## A. Ordinary full CP and ACP

---

**Algorithm 3** Full CP - Ordinary

---

```

1: for  $x$  in test points do
2:    $\theta_{Z \cup \{\hat{z}\}} = \underset{\hat{\theta} \in \Theta}{\operatorname{argmin}} R(Z \cup \{\hat{z}\}, \hat{\theta})$ 
3:   for  $\hat{y} \in \mathcal{Y}$  do
4:      $\hat{z} = (x, \hat{y})$ 
5:     for  $z_i \in Z \cup \{\hat{z}\}$  do
6:        $\alpha_i = \ell(z_i, \theta_{Z \cup \{\hat{z}\}})$ 
7:     end for
8:      $p_{(x, \hat{y})} = \frac{\#\{i=1, \dots, N+1 : \alpha_i \geq \alpha_{N+1}\}}{N+1}$ 
9:     If  $p_{(x, \hat{y})} > \varepsilon$ , include  $\hat{y}$  in prediction set  $\Gamma^\varepsilon$ 
10:   end for
11: end for

```

---

Algorithm 3 shows the full CP algorithm constructed for a nonconformity measure defined on an ordinary scheme. ACP with the ordinary prediction can be defined similarly to the deleted one as follows. Once again, we can use the direct or indirect approach.

**Indirect approach.** Let  $\tilde{\theta}_{Z \cup \{\hat{z}\}} \equiv \theta_Z + I_{\theta_Z}(\hat{z})$ . Then:

$$\alpha_i \approx \ell(z_i, \tilde{\theta}_{Z \cup \{\hat{z}\}}). \quad (7)$$

**Direct approach.**

$$\begin{aligned} \alpha_i &\approx \tilde{\ell}(z_i, \theta_{Z \cup \{\hat{z}\}}) \\ &\equiv \ell(z_i, \theta_Z) + I_\ell(z_i, \hat{z}) \end{aligned} \quad (8)$$

Observe that the only difference w.r.t. ACP (deleted) is that here we only need to add the influence of  $\hat{z}$ ; that is, we do not need to remove the influence of  $z_i \in Z \cup \{\hat{z}\}$ . This spares the very costly LOO procedure of retraining the model, which makes this method significantly more computationally efficient.

## B. Proofs

We restate our main assumptions.

**Assumption 1.** For every  $z_i \in Z$ :

$$\ell(z_i, \theta_{Z \cup \{\hat{z}\} \setminus \{z_i\}}) \leq \ell(z_i, \theta_Z).$$

**Assumption 2.** For every  $z_i \in Z$ :

$$I_\ell(z_i, \hat{z}) \geq I_\ell(z_i, z_i).$$

### B.1. Direct approximation is better than indirect

**Lemma 1.** Assume that the loss  $\ell$  is convex and differentiable. Let  $\alpha_i = \ell(z_i, \theta_{Z \cup \{\hat{z}\} \setminus \{z_i\}})$ . Then:

$$|\tilde{\ell}(z_i, \theta_{Z \cup \{\hat{z}\} \setminus \{z_i\}}) - \alpha_i| \leq |\ell(z_i, \tilde{\theta}_{Z \cup \{\hat{z}\} \setminus \{z_i\}}) - \alpha_i|.$$

That is, the direct method (Equation 6) gives a better approximation than the indirect one (Equation 5).

*Proof.* From Assumption 1 and Assumption 2 one easily derives that:

$$\begin{aligned} \alpha_i &= \ell(z_i, \theta_{Z \cup \{\hat{z}\} \setminus \{z_i\}}) \\ &\leq \ell(z_i, \theta_Z) + I_\ell(z_i, \hat{z}) - I_\ell(z_i, z_i) \\ &= \tilde{\ell}(z_i, \theta_{Z \cup \{\hat{z}\} \setminus \{z_i\}}) \end{aligned}$$

If a function  $g(x)$  is convex and differentiable, it lies above its tangent at any point:  $g(x) \geq g(y) + g'(y)(x - y)$  for all  $x, y$  in its domain. Observe that  $\tilde{\ell}(z_i, \theta_{Z \cup \{\hat{z}\} \setminus \{z_i\}})$ , if considered as a function in the model, is the tangent of  $\ell(z_i, \theta_{Z \cup \{\hat{z}\} \setminus \{z_i\}})$ :

$$\begin{aligned}\tilde{\ell}(z_i, \theta_{Z \cup \{\hat{z}\} \setminus \{z_i\}}) &= \ell(z_i, \theta_Z) + I_\ell(z_i, \hat{z}) - I_\ell(z_i, z_i) \\ &= \ell(z_i, \theta_Z) + \nabla_\theta \ell(z_i, \theta_Z)(I_{\theta_Z}(\hat{z}) - I_{\theta_Z}(z_i)) \\ &\leq \ell(z_i, \theta_Z + I_{\theta_Z}(\hat{z}) - I_{\theta_Z}(z_i)) \\ &= \ell(z_i, \tilde{\theta}_{Z \cup \{\hat{z}\} \setminus \{z_i\}})\end{aligned}$$

Recapping,

$$\alpha_i \leq \tilde{\ell}(z_i, \theta_{Z \cup \{\hat{z}\} \setminus \{z_i\}}) \leq \ell(z_i, \tilde{\theta}_{Z \cup \{\hat{z}\} \setminus \{z_i\}}),$$

from which the result follows.  $\square$

## B.2. ACP consistency

To prove Theorem 2 we exploit the following result by Giordano et al. (2019): Let  $\tilde{\theta}_{Z \setminus \{z_i\}} = \theta_Z - I_\theta(z_i, z_i)$  be the approximation of  $\theta_{Z \setminus \{z_i\}}$  obtained from Equation 3.

**Theorem 4** (Consistency of  $\tilde{\theta}_{Z \setminus \{z_i\}}$  (Giordano et al., 2019)). *Assume that:*

- For all  $\theta \in \Theta$  and all  $z_i \in Z$ ,  $\nabla_\theta \ell(z_i, \theta)$  is continuously differentiable in  $\theta$ .
- For all  $\theta \in \Theta$ , the Hessian  $H_\theta$  is non-singular with  $\sup_{\theta \in \Theta} \|H_\theta^{-1}\|_{op} \leq C_{op} < \infty$ .
- $\exists$  finite constants  $C_g$  and  $C_h$  s.t.:  $\sup_{\theta \in \Theta} \frac{1}{\sqrt{N}} \|\nabla_\theta \ell(z, \theta)\|_2 \leq C_g$  and  $\sup_{\theta \in \Theta} \frac{1}{\sqrt{N}} \|\nabla_\theta^2 \ell(z, \theta)\|_2 \leq C_h$ .
- Let  $h(\theta) = \frac{\partial \nabla_\theta \ell(z_i, \theta)}{\partial \theta}$ . There exists  $\Delta_\theta > 0$  and a finite constant  $L_h$  such that  $\|\theta - \theta_Z\|_2 \leq \Delta_\theta$  implies that  $\frac{\|h(\theta) - h(\theta_Z)\|_2}{\sqrt{N}} \leq L_h \|\theta - \theta_Z\|_2$ .

Then for every  $N$  there is a constant  $C$  s.t., for every  $z_i \in Z$ :

$$\begin{aligned}\|\tilde{\theta}_{Z \setminus \{z_i\}} - \theta_{Z \setminus \{z_i\}}\|_2 &\leq C \frac{\|g\|_\infty^2}{N^2} \\ &\leq C \frac{\max\{C_g, C_h\}^2}{N}\end{aligned}$$

(Note, the result by Giordano et al. is stated more generally for the case of leave  $k$  out; we only report its LOO version. Also, the general case requires 2 further assumptions, which we omit as they are always satisfied for LOO.)

We now restate and prove the consistency of ACP.

**Theorem 2** (Consistency of approximate full CP). *Suppose  $\ell$  is  $K$ -Lipschitz. Then for every  $N$  there is a constant  $C$  such that for every  $z_i \in Z \cup \{\hat{z}\}$ :*

$$|\tilde{\ell}(z_i, \theta_{Z \cup \{\hat{z}\} \setminus \{z_i\}}) - \alpha_i| \leq KC \frac{\max\{C_g, C_h\}^2}{N}.$$

*Proof.* First, from Theorem 4 (Giordano et al., 2019) we have that, for every  $N$  there exists constants  $C$  and  $C'$  such that:

$$\begin{aligned}\|\theta_{Z \cup \{\hat{z}\}} - I_\theta(z_i) - \theta_{Z \cup \{\hat{z}\} \setminus \{z_i\}}\|_2 &\leq C \frac{\max\{C_g, C_h\}^2}{N} \\ \|\theta_{Z \cup \{\hat{z}\}} - I_\theta(\hat{z}) - \theta_Z\|_2 &\leq C' \frac{\max\{C_g, C_h\}^2}{N};\end{aligned}$$

observe that the second expression is obtained by removing  $\hat{z}$  from the training data of a model trained on  $Z \cup \hat{z}$ .  $\square$

Fix  $z_i \in Z \cup \{\hat{z}\}$ .

$$\begin{aligned}
 |\tilde{\ell}(z_i, \theta_{Z \cup \{\hat{z}\} \setminus \{z_i\}}) - \ell(z_i, \theta_{Z \cup \{\hat{z}\} \setminus \{z_i\}})| &\leq |\ell(z_i, \tilde{\theta}_{Z \cup \{\hat{z}\} \setminus \{z_i\}}) - \ell(z_i, \theta_{Z \cup \{\hat{z}\} \setminus \{z_i\}})| \\
 &= |\ell(z_i, \tilde{\theta}_{Z \cup \{\hat{z}\} \setminus \{z_i\}}) - \ell(z_i, \theta_{Z \cup \{\hat{z}\} \setminus \{z_i\}})| \\
 &\leq K \|\tilde{\theta}_{Z \cup \{\hat{z}\} \setminus \{z_i\}} - \theta_{Z \cup \{\hat{z}\} \setminus \{z_i\}}\|_2 \\
 &= K \|\theta_Z + I_\theta(\hat{z}) - I_\theta(z_i) - \theta_{Z \cup \{\hat{z}\} \setminus \{z_i\}}\|_2 \\
 &\leq K \|\theta_{Z \cup \{\hat{z}\}} - I_\theta(z_i) - \theta_{Z \cup \{\hat{z}\} \setminus \{z_i\}}\|_2 + \|\theta_{Z \cup \{\hat{z}\}} - I_\theta(\hat{z}) - \theta_Z\|_2 \\
 &\leq K(C + C') \frac{\max\{C_g, C_h\}^2}{N}
 \end{aligned}$$

First step applies Lemma 1, third step uses Lipschitz continuity, fourth step uses triangle inequality, and the final step uses Theorem 4.

### B.3. Dependence on the regularization parameter $\lambda$

Our result on the effect of the regularization parameter on the approximation error of ACP (Theorem 3) is an extension of a result by Koh et al. (2019) on the approximation error of IF for LOO.

#### BACKGROUND ON RESULT BY KOH ET AL. (2019)

The LOO loss can be written as

$$\ell(z_i, \theta_{Z \setminus \{z_i\}}) = \ell(z_i, \theta_Z) - I_\ell^*(z_i, z_i) \approx \ell(z_i, \theta_Z) - I_\ell(z_i, z_i),$$

where  $I_\ell^*(z_i, z_i)$  is defined to be the true influence of training point  $z_i \in Z$  on the loss of the model at  $z_i$ . For simplicity, we omit the arguments of  $I_\ell$  when clear from the context. In the following, we assume  $\theta$  is the minimizer of an ERM problem with regularization parameter  $\lambda$ .

Koh et al. (2019) decompose the influence function error into Newton-actual error ( $E_A$ ) and Newton-influence error ( $E_I$ ):

$$I_\ell^* - I_\ell = E_A - E_I$$

with  $E_A \equiv I_\ell^* - I_\ell^N$ , and  $E_I = I_\ell^N - I_\ell$ .

Koh et al. (2019) show that  $E_A$  decreases with  $\mathcal{O}(\frac{1}{\lambda^3})$ , and they observed that its value tends to be negligible in practice.

**Proposition 5** (Koh et al. (2019)). *Assume that  $\ell$  is  $C_f$ -Lipschitz and that the Hessian is  $C_H$ -Lipschitz. Further, assume the third derivative of  $\ell$  exists and that it is bounded in norm by  $C_{f,3}$ . The influence on the self-loss is such that:*

$$I_\ell(z_i) + E_{f,3} \leq I_\ell^N(z_i) \leq \left(1 + \frac{3\sigma_{max}}{2\lambda} + \frac{\sigma_{max}^2}{2\lambda^2}\right) I_\ell(z_i) + E_{f,3}(z_i).$$

Furthermore:

$$|E_{f,3}(z_i)| \leq \frac{C_{f,3} C_\ell^3}{6(\sigma_{min} + \lambda)^3}.$$

#### EXTENSION TO ACP

If we assume  $E_A$  to be negligible, we obtain that  $I_\ell^* \approx I_\ell^N$ . Further, ignoring  $\mathcal{O}(\lambda^{-3})$  terms, Proposition 5 gives:

$$I_\ell \leq I_\ell^* \leq g(\lambda) I_\ell,$$

that is (by subtracting each term from  $\ell(z_i, \theta_Z)$ ):

$$\ell(z_i, \theta_Z) - g(\lambda) I_\ell(z_i, z_i) \leq \ell(z_i, \theta_{Z \setminus \{z_i\}}) \leq \ell(z_i, \theta_Z) - I_\ell(z_i, z_i) = \tilde{\ell}(z_i, \theta_{Z \setminus \{z_i\}}).$$

Note, however, that this result only applies to the LOO loss. We make the following simplifying assumption to extend the above result to ACP.

**Assumption 4.** For all  $z_i$  and  $\hat{z}$ :

$$I_\ell^*(z_i, \hat{z}) \approx I_\ell(z_i, \hat{z})$$

We can now restate and prove our result.

**Theorem 3** (Approximation goodness w.r.t. regularizer). *Suppose the model is trained via ERM with regularization parameter  $\lambda$ . Under the assumptions of Proposition 5, Assumption 4, and neglecting  $\mathcal{O}(\lambda^{-3})$  terms, we have the following cone constraint between the true nonconformity measure  $\alpha_i = \ell(z_i, \theta_{Z \cup \{\hat{z}\} \setminus \{z_i\}})$  and its direct approximation  $\tilde{\ell}(z_i, \theta_{Z \cup \{\hat{z}\} \setminus \{z_i\}}) \equiv \ell(z_i, \theta_Z) + I_\ell(z_i, \hat{z}) - I_\ell(z_i, z_i)$ :*

$$\begin{aligned} \ell(z_i, \theta_Z) + I_\ell(z_i, \hat{z}) - g(\lambda)I_\ell(z_i, z_i) \\ \leq \alpha_i \leq \tilde{\ell}(z_i, \theta_{Z \cup \{\hat{z}\} \setminus \{z_i\}}) \end{aligned}$$

with  $g(\lambda) = (1 + 3\sigma_{max}/2\lambda + \sigma_{max}^2/2\lambda^2)$ , where  $\sigma_{max}$  is the maximum eigenvalue of the Hessian  $H$ .

*Proof.* Koh et al. show that (ignoring  $\mathcal{O}(\lambda^{-3})$  terms):

$$I_\ell(z_i) \leq I_\ell^N(z_i) \leq \left(1 + \frac{3\sigma_{max}}{2\lambda} + \frac{\sigma_{max}^2}{2\lambda^2}\right) I_\ell(z_i).$$

(For a definition of all the terms please refer to Appendix B.3.) Ignoring  $\mathcal{O}(\lambda^{-3})$  terms, we apply this to the loss:

$$\ell(z_i, \theta_Z) - g(\lambda)I_\ell(z_i, z_i) \leq \ell(z_i, \theta_{Z \setminus \{z_i\}}) \leq \ell(z_i, \theta_Z) - I_\ell(z_i, z_i)$$

We apply this to the augmented training set  $Z \cup \{\hat{z}\}$  (now  $z_i$  ranges in  $Z \cup \{\hat{z}\}$ ):

$$\ell(z_i, \theta_{Z \cup \{\hat{z}\}}) - g(\lambda)I_\ell(z_i, z_i) \leq \ell(z_i, \theta_{Z \cup \{\hat{z}\} \setminus \{z_i\}}) \leq \ell(z_i, \theta_{Z \cup \{\hat{z}\}}) - I_\ell(z_i, z_i).$$

By using Assumption 4, replace  $\ell(z_i, \theta_{Z \cup \{\hat{z}\}})$  with  $\ell(z_i, \theta_Z) + I_\ell(z_i, \hat{z})$ . This concludes the proof.  $\square$

## C. Experimental details

### C.1. Datasets

Follows a brief description of the used datasets and the applied pre-processing.

- **MNIST**: we use 60,000 images for training and 10,000 for testing from the MNIST dataset (LeCun, 1998) – from which we take the first 100 test points. The 28×28 grayscale images represent handwritten digits between 0 and 9. In all settings except the CNN, these images are standardized in the interval [0, 1] by dividing the pixel intensities by 255.
- **CIFAR-10**: we use 50,000 images for training and 10,000 for testing from the CIFAR-10 dataset – from which we take the first 100 test points. These correspond to images from 10 mutually exclusively classes. We also standardize them in the interval [0, 1] (except in setting CNN).
- **US Census**: we use the ACSIncome data for the state of New York from the US Census dataset (Ding et al., 2021). Each data point represents an individual above the age of 16, who reported usual working hours of at least 1 hour per week in the past year, and an income of at least \$100. Ten features characterize each point, and the task consists of predicting whether the individual's income is above \$50,000. We split the dataset of 103,021 points and keep the 90% (92718) for training. We take 100 test points from the remaining.

## C.2. Implementation details

We use dense layers with Rectified Linear Units (ReLU) as nonlinear activation functions in all the models. We make explicit the width and depth for settings 20-10, 100, and 100-50-20 in the name (e.g., setting 20-10 is based on two layers with 20 and 10 neurons, in this order). All models are trained with Adam for a maximum of 200 epochs. We fix a learning rate of 0.001, minibatches of size 100, and an early stopping based on a 20% validation split. We also set a regularization  $\lambda = 10^{-5}$ . We use a cross-entropy loss function.

We use an autoencoder (AE) to reduce the dimensionality of MNIST and CIFAR-10 for settings 20-10, 100, 100-50-20, and LR. The AE uses a symmetric encoder-decode architecture with two dense layers of 128 and 64 neurons, separated by dropout with  $p = 0.2$  and ReLU activations.

We now give specific details of each setting:

- **20-10**: two layers with 20 and 10 neurons. The embedding size for the AE is 8.
- **100**: one layer with 100 neurons. Embedding size of 16.
- **100-50-20**: three layers with 100, 50, and 20 neurons. Embedding size of 32.
- **LR**: embedding size of 8.
- **CNN**: two convolutional layers with 16 and 32 kernels of size 5, respectively. They include a ReLU activation and max-pool layer with kernel size 4. A multilayer-perceptron makes the classification.

## C.3. Design choices for the methods

Here we comment on some design choices that we made when including the competing methods.

- **SCP**: we fix a calibration split of 20%, as advised in (Linusson et al., 2014). We obtain the nonconformity scores by fitting the model in the proper training set and computing the loss for the calibration data.
- **RAPS**: we fix a calibration split of 20%. We use the randomized version of the algorithm, and we do not allow zero sets (i.e., we use the default version in (Angelopoulos et al., 2020)). The randomized version, although slightly unstable, provides a less conservative coverage. The parameters 'kreg' and 'lamda' are picked in an optimal fashion that minimizes the prediction set size. We therefore compare ACP to the most efficient approach to RAPS.
- **CV+**: we set  $K = 5$  as the number of folds for the cross-validation.

## D. Fuzziness comparison

Table 3 shows the fuzziness of ACP and SCP on the US Census dataset. Results match the behavior observed for MNIST and CIFAR-10 (Section 5).

Model	US Census		
	ACP (D)	ACP (O)	SCP
20-10	0.1086	<b>0.0844</b>	0.1121 <sup>†</sup>
100	<b>0.1144</b>	0.1366	0.2173*
100-50-20	<b>0.0733</b>	0.0768	0.0741
LR	<b>0.0781</b>	0.0782	0.0885

Table 3. Fuzziness of ACP and SCP on US Census. A smaller fuzziness corresponds to more efficient prediction sets.

\*Differences in the AUC score are statistically significant compared to ACP (D). <sup>†</sup>Differences are significant compared to ACP (O).

## E. Further results

### E.1. Additional experiments with synthetic data

We run additional experiments on synthetic data to further support the theory in Section 3.2. Specifically, we show how ACP's p-values approximate full CP's as the training set increases, for different numbers of features and regularization strengths. We also compute the Kendall tau distance between the p-values rankings.

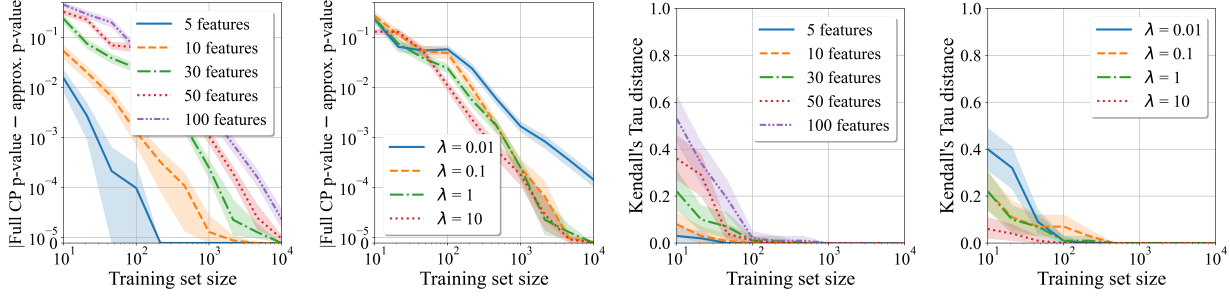


Figure 9. Additional experiments on synthetic data. We further support that ACP generates the same p-values as full CP as the training set increases.

## E.2. Additional motivating examples

We include additional motivating examples with specific instances from CIFAR-10 and MNIST.

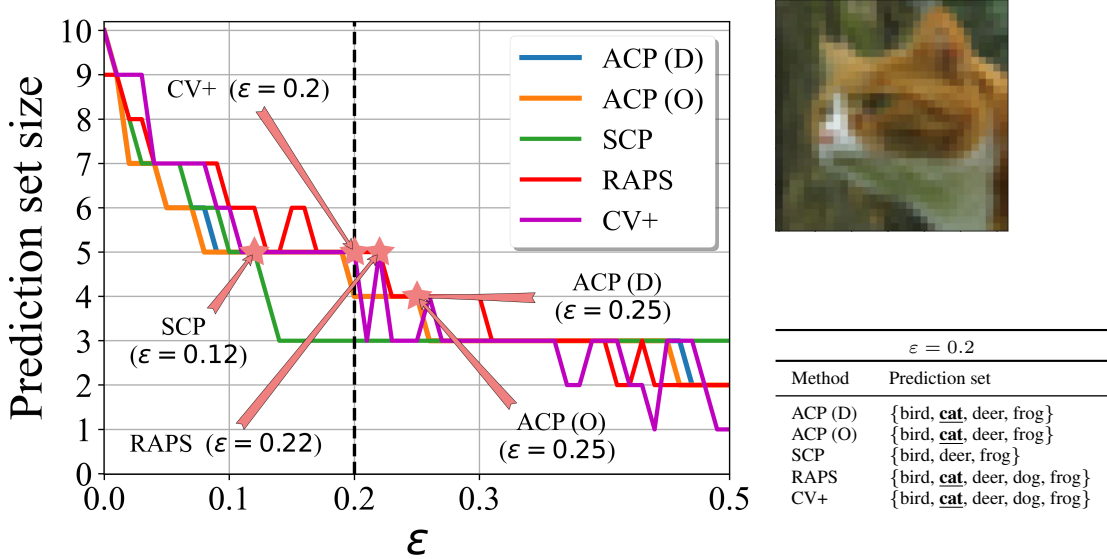


Figure 10. Prediction set size as a function of  $\varepsilon$  for a specific instance from CIFAR-10. We indicate with a star the point ( $\varepsilon$ ) at which each method starts containing the true label. ACP (D) and ACP (O) are the *fastest*, meaning that they include the true label earlier than the rest of methods (i.e., at higher  $\varepsilon$ ). For a typical significance  $\varepsilon = 0.2$ , the prediction sets generated by both methods are the smallest that contain the true label. RAPS and CV+ are more conservative, while SCP fails to include it.

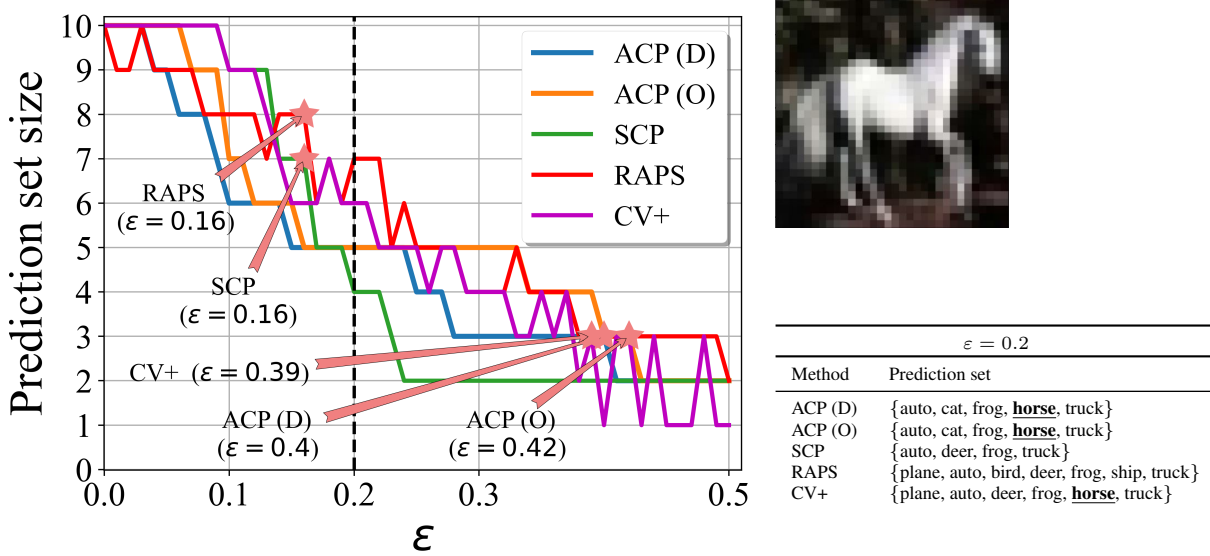


Figure 11. Additional motivating example in CIFAR-10. For a typical significance  $\varepsilon = 0.2$ , ACP (D) and ACP (O) yield the smallest prediction sets that contain the true label. ACP (D) and ACP (O) are the first to consider the true label.

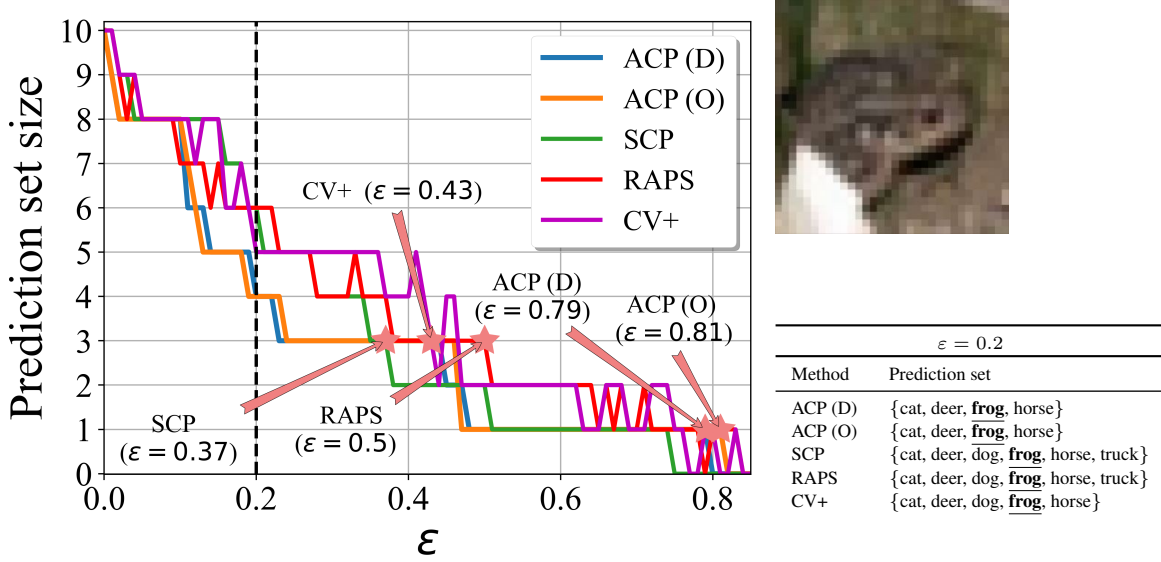


Figure 12. Additional motivating example in CIFAR-10. For a typical significance  $\varepsilon = 0.2$ , all methods include the true label, ACP (D) and ACP (O) yielding the smallest prediction sets. ACP (D) and ACP (O) are the first to consider the true label.

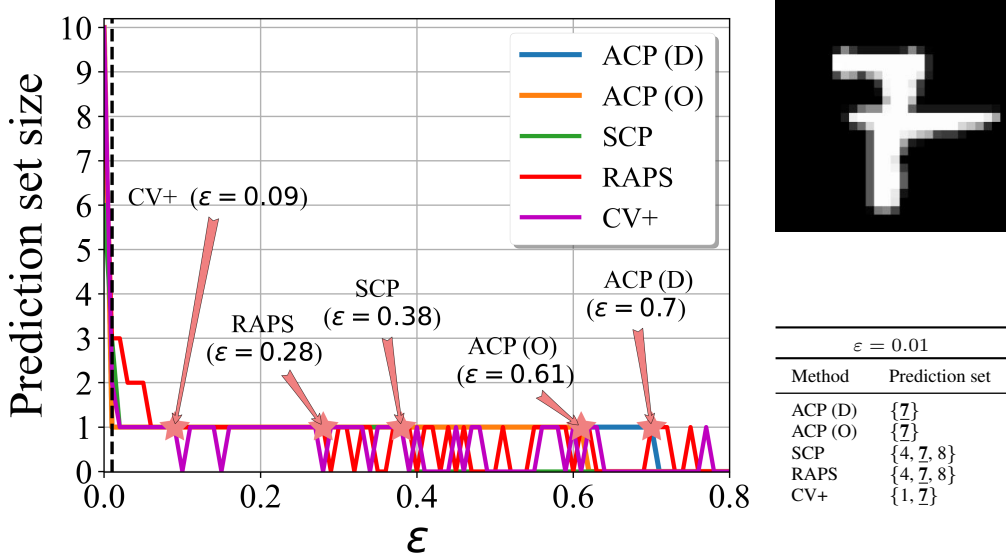


Figure 13. Additional motivating example in MNIST. For a typical significance  $\varepsilon = 0.01$ , all methods include the true label, ACP (D) and ACP (O) yielding the smallest prediction sets. ACP (D) and ACP (O) are also the first to consider the true label.

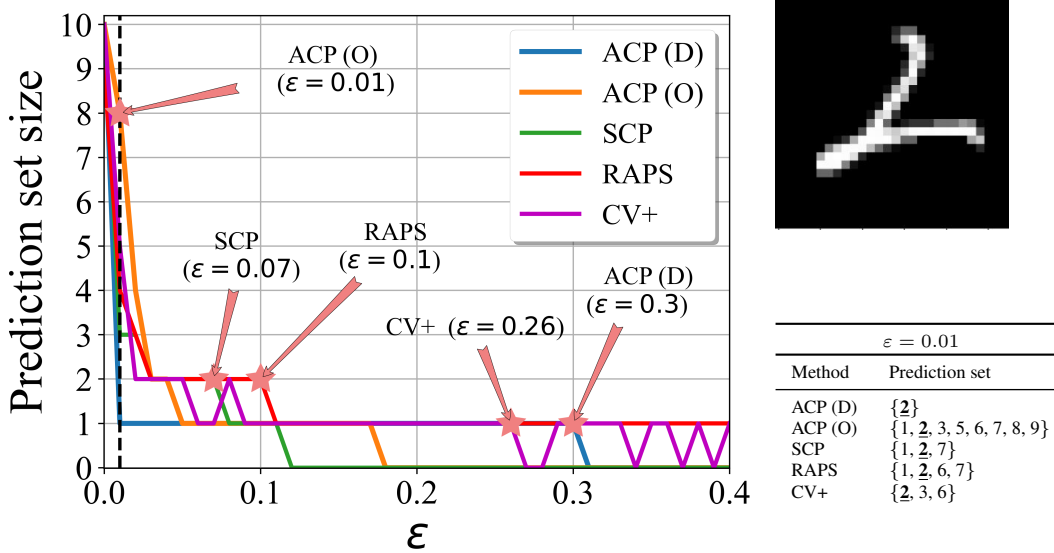


Figure 14. Additional motivating example in MNIST. For a typical significance  $\varepsilon = 0.01$ , all methods include the true label, ACP (D) yielding the smallest prediction sets. ACP (D) is the first method to consider the true label, followed by CV+. ACP (O) builds the largest set and is the *slowest* to consider the true label.

### E.3. Additional curves

Figure 15 plots the average prediction set size w.r.t the significance  $\varepsilon$  for all combinations of settings (20-10, 100, 100-50-20, LR, CNN) and datasets (MNIST, CIFAR-10, US Census).

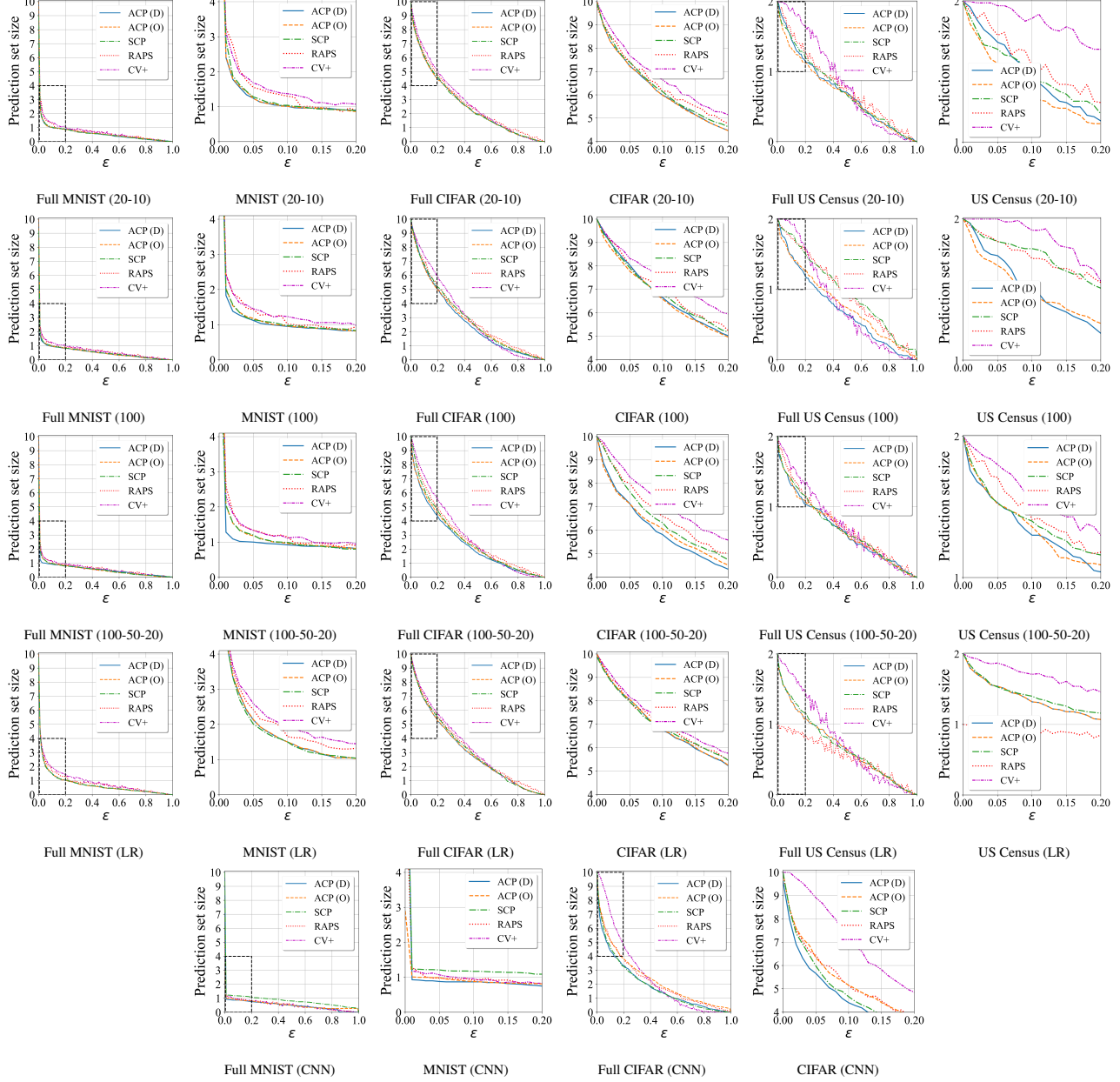


Figure 15. Average prediction set size w.r.t the significance level  $\varepsilon$  for all settings and datasets. We show both the full curve and the corresponding to the interval of interest  $\varepsilon \in [0, 0.2]$